ACS Photonics

Article

pubs.acs.org/journal/apchd5

A Universal Law for Plasmon Resonance Shift in Biosensing

Weihua Zhang*,†,‡ and Olivier J. F. Martin§

†College of Engineering and Applied Sciences and ‡National Laboratory of Solid State Microstructures, Nanjing University, Nanjing 210093, China

§Nanophotonics and Metrology Laboratory, EPFL, Lausanne 1015, Switzerland

Supporting Information

ABSTRACT: We derive an explicit expression for the resonance frequency shift for a subwavelength plasmonic nanocavity upon the adsorption or trapping of a single nanoparticle using rigorous perturbation theory. It reveals a simple linear dependence of the resonance frequency shift on the product of the local field intensity of a resonance mode, the material dispersion factor $d\omega_i/d\varepsilon$ of the nanocavity, and the polarizability of the nanoparticle. To verify this linear relation, we numerically simulate the nanoparticle-induced resonance shifts for subwavelength ellipsoids, rods, rod pairs, and split rings with different sizes and materials, and a very good agreement is found between the theory and the numerical results. Moreover, we discuss this approach from the energy perspective and find that the linear relation can be understood in the context of optical trapping. This work not only reveals the underlining physics of near-field couplings in plasmonic nanocavities but also provides theoretical guidelines for the design of ultrasensitive nanosensors.

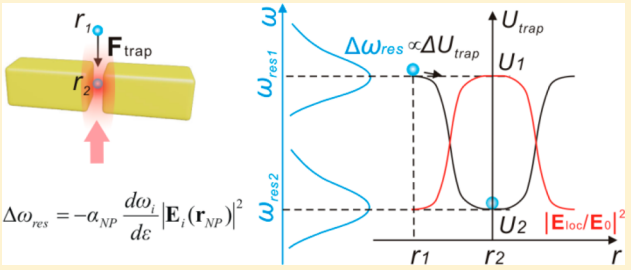

KEYWORDS: *plasmonics, sensing, nanocavity, perturbation theory*

The resonance frequency of a plasmonic nanocavity can be altered by a minute modification of its optical near-field, caused for example by the optical trapping of nanoparticles (NPs)[1] or the absorption of molecules.[2,3] This high spectral sensitivity makes plasmonic nanocavities a very attractive platform for building active optical nanodevices, such as switches,[4] modulators,[5−7] tunable antennas,[8] and nanosensors.[9] To date, many experimental works have dealt with the resonance frequency shift phenomenon of different plasmonic nanostructures, including nanoprisms,[10] nanorods,[2] nanocubes,[11,12] nanoshells,[13,14] and nanobranches,[15] with the goal of finding the best plasmonic nanosensor and, eventually, achieving integrated high-throughput sensing devices[16,17] with single-molecule sensitivity.[2,9] Meanwhile, theoretical endeavors have also been reported on the sensitivity and the limit of detection for plasmonic biosensors.[18−20] However, to date, there is still lack of a comprehensive yet simple general theory that can address fundamental questions such as what determines the sensitivity of a plasmonic nanosensor and which structure gives the best sensitivity (largest resonance frequency shift) upon the presence of a single NP or molecule. A general theory that can provide an explicit link of the sensitivity to material and geometrical parameters is therefore required for understanding, analyzing, and further developing plasmonic nanostructure-based active devices, especially sensors.

In order to interpret the perturbation-induced resonance shift of plasmonic nanostructures quantitatively, one often uses the theory of dielectric microcavity systems, in which the resonance frequency shift $\Delta\omega_i$ can be explicitly expressed as the shift of the cavity eigenmode i:[21−24]

$$\Delta\omega_i = -\frac{\omega_i}{2}\frac{\int \mathrm{d}\mathbf{r}\ \Delta\varepsilon(\mathbf{r})|E(\mathbf{r})|^2}{\int \mathrm{d}\mathbf{r}\ \varepsilon(\mathbf{r})|E(\mathbf{r})|^2} \quad (1)$$

Equation 1 explains the linear relation between resonance frequency shift and the local field intensity. However, strictly speaking, it is only applicable to structures made of nondispersive materials. For nanostructures made of dispersive materials, particularly plasmonic nanocavities, the denominator $\int \mathrm{d}\mathbf{r}\ \varepsilon(\mathbf{r})|\mathbf{E}(\mathbf{r})|^2$ in eq 1 can vanish,[25] which will lead to an unphysically large value for the resonance frequency.[26]

In this work, we develop a general theory for the resonance shift of dispersive plasmonic nanocavities using the eignenmode method, which we recently established based on Green's tensor technique.[27−29] Previously, it was shown that the scattered fields of a deep subwavelength structure can be decomposed into a series of eigenmodes, which are associated with dielectric constant eigenvalues.[27−30] In this work, we will utilize this eigenmode method and build a rigorous perturbation theory to derive an explicit expression for the NP-induced resonance frequency shifts of plasmonic nanocavities.

The paper is organized as follows. First, we derive the general expression for the resonance frequency shift of a nanocavity using the eigenmode technique. Then, we verify the validity of

Received: September 28, 2014
Published: December 1, 2014

this result on various types of plasmonic nanocavities with numerical experiments and discuss the influences of the local field intensity, the material dispersion, and the cavity quality factor on the resonance shift. Finally, we investigate the resonance frequency shift in the context of optical trapping, which provides a simple illustration of the resonance shift in the perspective of energy conservation.

PERTURBATION THEORY FOR THE RESONANCE MODES OF PLASMONIC NANOCAVITIES

The system under study is shown in Figure 1a. It consists of a plasmonic nanocavity and an NP. When the NP moves into the

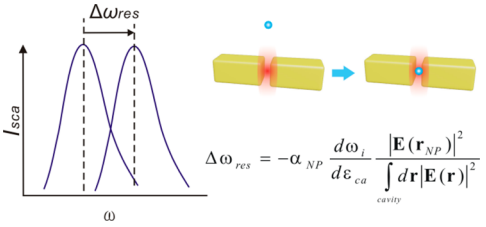

Figure 1. Sketch of the resonance shift phenomenon for a plasmonic nanocavity induced by the perturbation from a single NP.

near-field zone of the nanocavity, the resonance frequency ω_{res} will shift by $\Delta\omega_{res}$ due to near-field coupling. In this section, we derive a simple expression for $\Delta\omega_{res}$ using perturbation theory with the help of Green's tensor technique.

Eigenmodes of Nanocavities. Localized plasmon resonances of a plasmonic nanocavity can be viewed as the eigenmodes of the structure under the Bergman spectral respresentation.[27] We start from the Lippmann−Schwinger equation, which describes the scattering problem for electromagnetic fields:[31]

$$\mathbf{E}(\mathbf{r}) = \mathbf{E}_{ext}(\mathbf{r}) + \int_{cavity} d\mathbf{r}'\, G_0(\mathbf{r}, \mathbf{r}')\cdot\Delta\varepsilon(\mathbf{r}')k_0^2\, \mathbf{E}(\mathbf{r}') \tag{2}$$

where $\Delta\varepsilon = \varepsilon_{ca} - \varepsilon_{bg}$ is the permittivity contrast between the scatter (nanocavity in this work) and the background medium, $\mathbf{E}_{ext}$ is the external field, $\mathbf{G}_0$ is the free-space Green's tensor, and k_0 is the wavenumber in the background medium. Let us define the material parameter, $s = 1/\Delta\varepsilon$, inner product,

$$\langle \mathbf{E}_i|\mathbf{E}_j\rangle = \int_{cavity} d\mathbf{r}\, \mathbf{E}_i(\mathbf{r})^*\cdot\mathbf{E}_j(\mathbf{r}) \tag{3}$$

and the linear operator

$$[\hat{\mathbf{G}}\mathbf{E}](\mathbf{r}) = \int_{cavity} d\mathbf{r}'\, \mathbf{G}_0(\mathbf{r}, \mathbf{r}')\cdot k_0^2\mathbf{E}(\mathbf{r}') \tag{4}$$

The homogeneous part of eq 2 (without external fields) becomes $\hat{\mathbf{G}}\mathbf{E} = s\mathbf{E}$. When the cavity is much smaller than the wavelength, the quasi-static approximation can be used, and eq 2 will own a complete set of orthonormal eigenmodes $\{\mathbf{E}_i, i = 1, 2, ...\}$, which fulfill the relation $\langle \mathbf{E}_i|\mathbf{E}_j\rangle = \delta_{ij}$ with real eigenvalues$\{s_i, i = 1, 2, ...\}$, which are located between −1 and 0.[27] The scattered field can be written as an expansion of the eigenmodes:

$$\mathbf{E} = \sum_i a_i\mathbf{E}_i \tag{5}$$

where

$$a_i = \frac{s}{s - s_i}\langle \mathbf{E}_{ext}|\mathbf{E}_i\rangle \tag{6}$$

Eigenmode i can be resonantly excited when the denominator in eq 6 approaches zero.

The singularities in eq 6 determine the resonance conditions for the nanocavity. Since s_i are located between −1 and 0, reaching the resonance condition requires a negative permittivity, which can be met by noble metals in the optical spectral range thanks to the optical response of the free electrons. Under resonance conditions, the free electrons oscillate collectively and produce the localized plasmon resonance. Because of the ohm losses of metal, $s/(s - s_i)$ has a Lorentzian function-like shape, and this phenomenon has been widely observed experimentally.[32]

Perturbation Theory. When a NP or protein molecule enters the near-field zone of a plasmonic nanocavity, the Lippmann−Schwinger equation of the perturbed system becomes

$$\mathbf{E}(\mathbf{r}) = \mathbf{E}_{ext}(\mathbf{r}) + 1/s\left(\int_{cavity} d\mathbf{r}'\, \mathbf{G}(\mathbf{r}, \mathbf{r}')\cdot\mathbf{E}(\mathbf{r}')k_0^2 + \frac{\varepsilon_{NP} - \varepsilon_{bg}}{\varepsilon_{ca} - \varepsilon_{bg}}\int_{NP} dr'\, \mathbf{G}(\mathbf{r}, \mathbf{r}')\cdot\mathbf{E}(\mathbf{r}')k_0^2\right) \tag{7}$$

Here, ε_{ca} and ε_{NP} are the permittivity of the nanocavity and perturbing NP, respectively. Assuming that the NP is much smaller than the nanocavity, the last term in eq 7 can be treated as a perturbation, and the eigenvalues and eigenmodes of the perturbed system become $s_i' = s_i + \Delta s_i$, and $\mathbf{E}_i' = \mathbf{E}_i + \Delta\mathbf{E}_i$. By applying a perturbation procedure, we obtain a simple expression for the first-order correction of the eigenvalue s_i (see the Supporting Information):

$$\Delta s_i = 4\pi {r_{NP}}^3\frac{1}{(\varepsilon_{ca} - \varepsilon_{bg})^2}\frac{\varepsilon_{NP} - \varepsilon_{bg}}{(\varepsilon_{NP} + 2\varepsilon_{bg})}|\mathbf{E}_i(\mathbf{r}_{NP})|^2 \tag{8}$$

Knowing that the polarizability of a spherical NP is $\alpha_{NP} = 4\pi {r_{NP}}^3[(\varepsilon_{NP} - \varepsilon_{bg})/(\varepsilon_{NP} + 2\varepsilon_{bg})]$ and finite difference of $s(\omega)$ is $\Delta s_i = -[1/(\varepsilon_{ca} - \varepsilon_{bg})^2](d\varepsilon_{ca}/d\omega_i)$, eq 8 can then be written as

$$\Delta\omega_i = -(d\omega_i/d\varepsilon_{ca})\alpha_{NP}|\mathbf{E}_i(\mathbf{r}_{NP})|^2 \tag{9}$$

where $\mathbf{r}_{NP}$ is the location of the perturbing NP or adsorbed molecule.

The mode profile $\mathbf{E}_i(\mathbf{r})$ can be obtained using the local electric field on the resonance frequency ω_i, which can be calculated with commonly used numerical simulation tools, such as finite-differences time-domain,[33] finite-elements method,[34] or Green's tensor technique.[31] Equation 6 shows that a_i becomes very large at the vicinity of the resonance condition for mode $\mathbf{E}_i$, and therefore

$$\mathbf{E}(\mathbf{r}) \approx a_i\mathbf{E}_i(\mathbf{r}) \tag{10}$$

Inserting eq 10 into $\langle \mathbf{E}_i|\mathbf{E}_i\rangle = 1$, we obtain $a_i = (\int_{cavity} d\mathbf{r}|\mathbf{E}(\mathbf{r})|^2)^{1/2}|_{\omega i}$, and $\mathbf{E}_i(\mathbf{r}) = \mathbf{E}(\mathbf{r}_{NP})/(\int_{cavity} d\mathbf{r}|\mathbf{E}(\mathbf{r})|^2)^{1/2}$. Equation 9 then becomes

$$\Delta\omega_i = -\alpha_{NP}\frac{d\omega_i}{d\varepsilon_{ca}}\frac{|\mathbf{E}(\mathbf{r}_{NP})|^2}{\int_{cavity} d\mathbf{r}\,|\mathbf{E}(\mathbf{r})|^2} \tag{11}$$

dx.doi.org/10.1021/ph500355d | ACS Photonics 2015, 2, 144−150

Equation 11 provides a general relation for the resonance frequency shifts for subwavelength cavities made of dispersive materials. It is universal, applicable to any type of dispersive nanocavities, irrespective of their size, shape, and material.

NUMERICAL VERIFICATION

Universality of the Resonance Shift Formula. To verify eq 11, we numerically simulated the resonance frequency shifts of nanocavities induced by an NP. In the simulation, nanocavities with different shapes, namely ellipsoids,[35] nanorods,[2] antennas (i.e., rod pair),[1] and split rings[36] made of different materials (Ag and Au) were coupled with a Si NP (5 nm in diameter) placed at different locations in the near-field zone of the nanocavities. The scattered fields were solved using Green's tensor technique by discretizing the nanocavities into 2 nm × 2 nm × 2 nm cubes. The simulated results are plotted in Figure 2a. The resonance behaviors of those nanostructures exhibit a great diversity, depending on the shape and material. No clear relation between the resonance shift and the shape, material, or resonance frequency can be observed.

To make a quantitative comparison between the numerical results and the theory, namely, eq 11, we extracted the resonance frequencies of the nanocavities with and without the Si NP by fitting their scattering spectra with a Lorentzian function and plotted the resonance shifts $\Delta\omega_{res}$ as a function of $-\alpha_{NP}(d\omega_i/d\varepsilon_{ca})(|\mathbf{E}(\mathbf{r}_{NP})|^2/\int_{cavity}d\mathbf{r}|\mathbf{E}(\mathbf{r})|^2$ for all nanocavities, as shown in Figure 2b. The plot includes 80 data points from 16 different nanocavities (four different shapes, two different sizes for each shape, and two different materials) perturbed by a Si NP at different locations for each nanocavity. The linear fitting result shows a slope of 1.07, with the correlation of 0.9927. This good agreement with eq 11 proves that the theory is universally applicable to subwavelength plasmonic nanocavities, independent of the shape, size, or material of the cavity.

Role of $|\mathbf{E}(\mathbf{r}_{NP})|^2$. An important property of eq 11 is that the resonance shift $\Delta\omega_{res}$ is linearly dependent on the local field intensity $|\mathbf{E}(\mathbf{r}_{NP})|$,[2] the key parameter for surface-enhanced spectroscopy.

To unveil the role of $|\mathbf{E}(\mathbf{r}_{NP})|^2$, plasmonic nanoantennas with different arm lengths were used as model systems. We calculated the resonant frequencies of plasmonic nanoantennas perturbed by a Si NP at different locations $\mathbf{r}_{NP}$ (i.e., with different local field intensities) and plotted in Figure 3a $\Delta\omega_{res}$ as a function of $|\mathbf{E}(\mathbf{r}_{NP})|^2$ for each antenna. Since $d\omega_i/d\varepsilon_{ca}$ and $\int_{cavity}d\mathbf{r}|\mathbf{E}(\mathbf{r})|^2$ are constant for the same nanoantenna, $\Delta\omega_{res}$ and $|\mathbf{E}(\mathbf{r}_{NP})|^2$ should be linearly dependent. Linear relations are indeed observed in Figure 3a, and fitting results reveal strong linear correlations: the correlation coefficient is 0.9992, 0.9995, 0.9997, and 0.9993 for the four plasmonic nanoantennas. In the plot, the slopes of the $\Delta\omega_{res}$ vs $|\mathbf{E}(\mathbf{r}_{NP})|^2$ curves are different because $d\omega_i/d\varepsilon_{ca}$ and $\int_{cavity}d\mathbf{r}|\mathbf{E}(\mathbf{r})|^2$ are different for nanoantennas with different arm lengths.

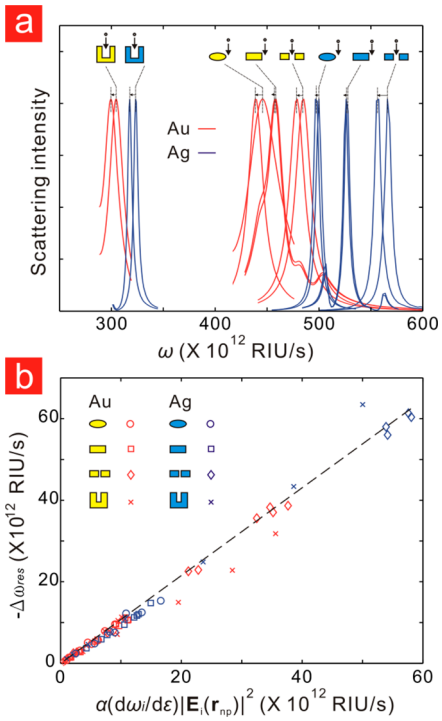

Figure 2. (a) Resonance frequency shift of plasmonic nanocavities induced by a single NP. (b) Resonance shift as a functitn of $\alpha_{NP}(d\omega_i/d\varepsilon)|\mathbf{E}_i(\mathbf{r}_{NP})|^2$ for different nanocavities. Simulation results for eight different types of plasmonic nanocavity structures are shown: namely, ellipsoid (40 nm long axis, 14 nm short axes), rod (10 nm × 10 nm cross-section, 26 nm long), nanoantenna (28 nm × 10 nm × 10 nm arm size, 10 nm gap), and split ring (10 nm × 10 nm wire cross-section, 32 nm × 30 nm outer dimension of the ring, 10 nm gap) made of Ag or Au. For each structure, we calculated the resonance shifts for five different NP locations $\mathbf{r}_{NP}$.

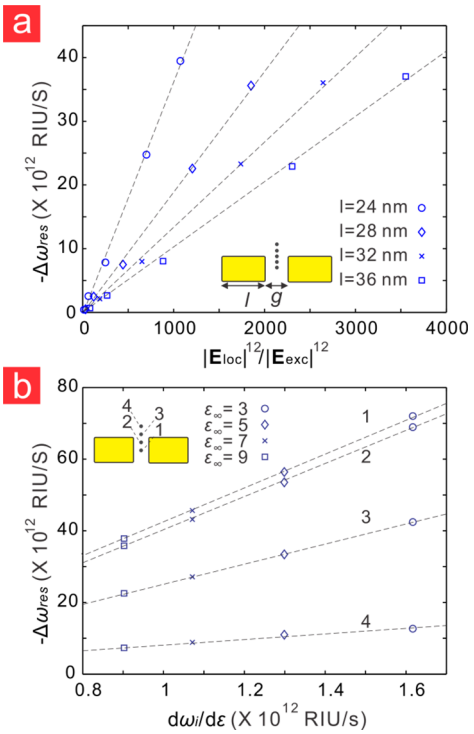

Figure 3. (a) Resonance shift $\Delta\omega_{res}$ as a function of the local field intensity $|\mathbf{E}(\mathbf{r}_{NP})|^2$ for plasmonic nanoantennas with different arm lengths (i.e., 24, 28, 32, and 36 nm). The dashed lines are the linear fitting results. (b) Resonance shift for plasmonic nanoantennas as a function of the material dispersion factor $d\omega_i/d\varepsilon_{ca}$. In the simulation, we kept the arm length of the nanoantenna constant (l = 32 nm) while varying the dispersion relation $\varepsilon(\omega)$ and the location $\mathbf{r}_{NP}$ of the NP, as sketched in the inset. The dashed lines are the linear fitting results. In (a) and (b), the gap size and cross-section of the antennas is 10 nm and 10 nm × 10 nm, respectively.

dx.doi.org/10.1021/ph500355d | ACS Photonics 2015, 2, 144−150

Role of the Material Dispersion Factor $d\omega_i/d\varepsilon_{ca}$. The key difference between eq 11 for dispersive nanocavities and eq 1 for dielectric (nondispersive) microcavities is $d\omega_i/d\varepsilon_{ca}$, a material dispersion-related factor. To verify the dependence on $d\omega_i/d\varepsilon_{ca}$, we need to (1) fix the value of $|\mathbf{E}(\mathbf{r}_{NP})|^2/\int_{cavity}d\mathbf{r}|\mathbf{E}(\mathbf{r})|^2$ in eq 11 (i.e., $|\mathbf{E}_i(\mathbf{r})|^2$ in eq 9), (2) change $d\omega_i/d\varepsilon_{ca}$, and then investigate the correlation between $d\omega_i/d\varepsilon_{ca}$ and $\Delta\omega_{res}$. To fix $|\mathbf{E}(\mathbf{r}_{NP})|^2/\int_{cavity}d\mathbf{r}|\mathbf{E}(\mathbf{r})|^2$, nanocavities with the same geometry were used. Since under the quasistatic approximation the resonance modes are solely determined by the geometry of a nanocavity, all the nanocavities share the same field distribution at the resonance frequency (i.e., same $|\mathbf{E}_i(\mathbf{r})|^2$). To vary the factor $d\omega_i/d\varepsilon_{ca}$, in this work we tune the permittivity of the nanocavity, which we describe with the Drude model: $\varepsilon(\omega) = \varepsilon_\infty - \omega_p^2/\omega(\omega + i\gamma)$, with ε_∞ the high-frequency permittivity, ω_p the plasma frequency, and γ the damping term.

In detail, we calculated the resonance shift $\Delta\omega_{res}$ for the antennas made of Drude metals with different ε_∞ (i.e., 3, 5, 7, and 9), and plotted in Figure 3b $\Delta\omega_{res}$ as a function of $d\omega_i/d\varepsilon_{ca}$. Strong linear correlation was found. The correlation coefficients for the four different perturbation locations $\mathbf{r}_{NP}$ are 0.9999, 0.9997, 1.0000, and 0.9907. These results directly demonstrate the importance of material dispersion in the response of plasmonic nanosensors and that it must be carefully taken into account to optimize them.

Role of Integral of the Eletric Field Intensity. The integral term $\int_{cavity}d\mathbf{r}|\mathbf{E}(\mathbf{r})|^2$ in eq 11 comes from the coefficient a_i in eq 5, which describes the excitation strength of the resonant mode $|\mathbf{E}_i\rangle$. Equation 6 shows that a_i is the product of two independent terms, the material-determined factor $s/(s - s_i)$ and the integral factor $\langle\mathbf{E}_{ext}|\mathbf{E}_i\rangle$. Term $s/(s - s_i)$ is decided by the material losses of the nanocavity and reaches its maximum value $\Delta\varepsilon_i/\varepsilon''$ under the resonance condition. The term $\langle\mathbf{E}_{ext}|\mathbf{E}_i\rangle$ describes the degree of overlap between the excitation field $\mathbf{E}_{ext}$ and the eigenmode $\mathbf{E}_i$. When a plane wave is used to excite the system, this term is proportional to the dipole moment of the nanocavity.[27] It is worth noting that the term $\langle\mathbf{E}_{ext}|\mathbf{E}_i\rangle$ scales with $V^{1/2}$, since $\mathbf{E}_i$ is scaled with $V^{1/2}$ (assuming that $\langle\mathbf{E}_i|\mathbf{E}_i\rangle$ is normalized). Therefore, the resonance frequency shifts are also proportional to V^{-1} (the smaller the cavity, the larger the resonance frequency shift).

NANOPARTICLE-INDUCED PLASMON RESONANCE SHIFT IN THE CONTEXT OF OPTICAL TRAPPING

The resonance frequency shift of a nanocavity upon perturbation by a nano-object is also associated with the optical forces and the change of energy in the system. It is therefore interesting to discuss eq 11 by considering the links between the resonance frequency, the optical forces, and the energy stored in the system. In this section, we will derive eq 9 from an energy perspective, then discuss the relation between resonance shift and optical trapping potential, and, finally, illustrate this relation for plasmonic antennas.

Resonance Shift vs Electric Field Energy. We have shown in the previous section that under the quasistatic approximation a nanocavity owns a complete set of orthornormal eigenmodes. Let us consider a single photon of the resonance mode i for a plasmonic nanocavity. When an NP enters its near-field zone, the NP will be polarized by the electric field. Under the first order of perturbation, the energy of the system will be changed by

$$\delta U_i = -\frac{1}{2}\mathbf{P}\cdot\mathbf{E}_i^*(\mathbf{r}_{NP}) = -\frac{1}{2}\alpha_{NP}|\mathbf{E}_i(\mathbf{r}_{NP})|^2 \tag{12}$$

Here, $\mathbf{P}$, α, and $\mathbf{r}_{NP}$ are the dipole moment, polarizability, and position of the NP, respectively. When α is positive, δU will be negative and trapping forces will be induced.

For a nanocavity made of dispersive material, the energy of the photon of mode i can be written as the sum of the field energy U_{cavity} stored in the metal cavity and that stored in the surrounding dielectric background, U_{bg}:[25,37]

$$U = U_{cavity} + U_{bg} = \frac{1}{2}\int_{cavity}\frac{\partial(\omega\varepsilon)}{\partial\omega}|\mathbf{E}_i(\mathbf{r})|^2 d\mathbf{r} + \frac{1}{2}\int_{bg}\varepsilon|\mathbf{E}_i(\mathbf{r})|^2\, d\mathbf{r} \tag{13}$$

In eq 13, $^1/_2\int_{cavity}\partial(\omega\varepsilon)/\partial\omega|\mathbf{E}|^2\, d\mathbf{r}$ is used instead of $\int_{cavity}d\mathbf{r}|\mathbf{E}(\mathbf{r})|^2$ because of the dispersion of the metal.[37] When the resonance frequency ω_i shifts by $\delta\omega$, the energy of the system will be changed by (see Supporting Information)

$$\delta U = \frac{1}{2}\delta\omega_i\frac{\partial\varepsilon_{ca}}{\partial\omega}\bigg|_{\omega_i} \tag{14}$$

Comparing eq 12 with eq 14, we obtain $\Delta\omega_i = -(d\omega_i/d\varepsilon_{ca})\alpha_{NP}|\mathbf{E}_i(\mathbf{r}_{NP})|^2$, which exactly corresponds to what was derived in the previous section using the rigorous perturbation theory.

From the above discussion, we learn that the dispersion term $d\omega_i/d\varepsilon_{ca}$ originates from the expression of electric field energy in dispersive materials $(d\omega_i/d\varepsilon_{ca})|\mathbf{E}|^2$, which is different from the case of dielectric materials: $\varepsilon|\mathbf{E}|^2$.

It is worth mentioning that, using the above approach, eqs 9 and 11 can be easily extended to the case of a thin adsorption layer around the cavity (entirely coated or partially coated), the most relevant case for biosensing. For a thin dielectric adsorbed layer with permittivity ε_{pert}, eq 12 becomes $\delta U_i = -^1/_2\int_{pert}d\mathbf{r}(\varepsilon_{pert} - \varepsilon_{bg})|\mathbf{E}_i(\mathbf{r})|^2$, and we have the resonance shift

$$\delta\omega_i = -(d\omega_i/d\varepsilon_{ca})\int_{pert}d\mathbf{r}(\varepsilon_{pert} - \varepsilon_{bg})|\mathbf{E}_i(\mathbf{r})|^2 \tag{15}$$

Optical Potential vs Resonance Shift. The above discussion unveils the relation between resonance frequency shift $\Delta\omega_{res}$ and the system's energy change, δU, which is directly linked to optical forces.

For a small NP, the optical forces are $\mathbf{F}(\mathbf{r}_{NP}) = {}^1/_2\alpha\nabla|\mathbf{E}(\mathbf{r}_{NP})|^2$, and the trapping potential can then be defined as

$$U_{trap}(\mathbf{r}_{NP}) = -\int_\infty^{r_{NP}}\mathbf{F}(\mathbf{r})\, d\mathbf{r} = \frac{1}{2}\alpha|\mathbf{E}(\mathbf{r}_{NP})|^2 \tag{16}$$

Comparing eq 16 with eq 11, we have

$$\Delta\omega_{res} \propto U_{trap}(\mathbf{r}_{NP}) \tag{17}$$

This linear relation between the optical trapping potential and the associated resonance shift has indeed been observed in previously reported optical trapping experiments with sub-wavelength optical antennas.[1] In that work, successive resonance shifts with different magnitudes were observed when two Au NPs were trapped at two different locations (e.g., the nanogap and the extremity of the plasmonic nanoantenna), corresponding to two different trapping potentials (see Figure 2b in ref 1).

To illustrate the optical trapping-induced resonance shift described by eq 16, we numerically simulated with Green's

dx.doi.org/10.1021/ph500355d | ACS Photonics 2015, 2, 144−150

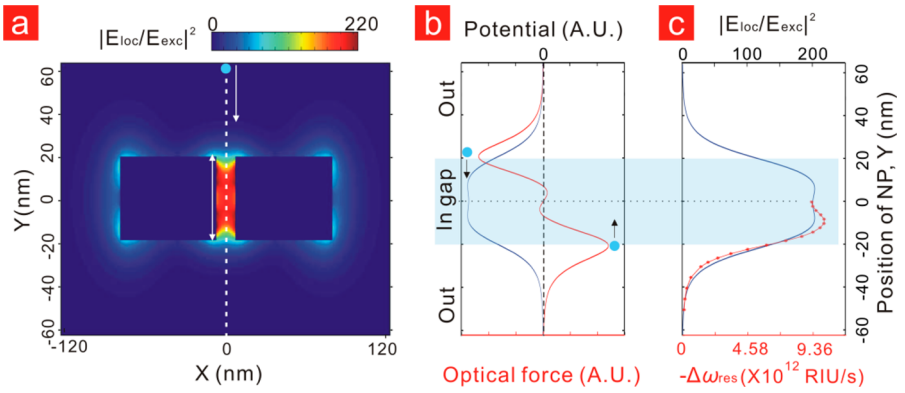

Figure 4. Relation between optical trapping forces, trapping potential, and associated resonance frequency shifts for a plasmonic nanoantenna (60 nm × 40 nm × 40 nm arm, 25 nm gap). (a) Local field intensity map for a plasmonic nanoantenna. (b) Optical trapping potential, U_{trap}, and optical forces, **F**, of a Au NP (10 nm in diameter) along the dashed line in (a). (c) Optical trapping potential U_{trap} and trapping-induced resonance frequency shift $\Delta\omega_{res}$ of the nanoantenna along the dashed line in (a).

tensor technique a plasmonic nanoantenna with a 25 nm gap coupled to a 10 nm Au NP. In detail, first, the field distribution of the antenna without NP was simulated, as shown in Figure 4a. Electric fields are highly enhanced and are homogeneous inside the nanogap; at the edge of the nanogap, the field intensity varies rapidly and drops to half of its maximum in just a few nanometers. Using this field distribution, trapping forces **F** and trapping potential U_{trap} along the axis crossing the antenna center were calculated and plotted in Figure 4b. To calculate the resonance shift caused by the NP, we placed the NP at different locations along the *y*-axis (i.e., the central axis along the nanogap), calculated the resonance spectra of the coupled system, and plotted in Figure 4c the resonance frequency as a function of the location of the NP. The profiles of the U_{trap} vs $\mathbf{r}_{NP}$ curve and the $\Delta\omega_{res}$ vs $\mathbf{r}_{NP}$ curve fit to each other very well, providing a direct support for the linear relation between the local field enhancement and the resonance shift in eq 17.

There are slight discrepancies between the two curves in Figure 4b. They are caused by the two approximations used for deriving eq 17. First, only the first-order correction of the perturbation theory is implemented. Second, it is assumed that the field in the NP is homogeneous, whereas, in reality, the field generated by the nanoantenna can vary substantially over a 10 nm NP, particularly when it is located at the boundary of the gap.

Strategy for Designing Ultrasensitive Plasmonic Sensors. The universal relation that we have derived for the resonance shift $\Delta\omega_{res}$ provides general guidelines for designing ultrasenstive plasmonic sensors. Equations 9 and 11 indicate that the sensitivity of a plasmonic sensor, namely, $\Delta\omega_{res}$, to an external perturbation is determined by two factors, the dispersion factor, $d\omega_i/d\varepsilon_{ca}$, and the local electric field intensity distribution of the eigenmode, $|\mathbf{E}_i(\mathbf{r}_{NP})|^2$. In the following section, we discuss these two factors in details.

Let us exam the dispersion factor first. In the previous section, it has been pointed out that, for the same geometry, $|\mathbf{E}_i(\mathbf{r}_{NP})|^2$ stays constant, and the resonance shift is solely determined by the dispersion of the material. Consider a plasmonic nanostructure made of a Drude metal, $\varepsilon(\omega) = \varepsilon_\infty - \omega_p^2/\omega(\omega + i\gamma)$, where ω_p is the plasma frequency and γ is the damping constant. For simplicity, we assume $\gamma = 0$. If its resonance modes are associated with the eigenvalues $s_i = 1/(\varepsilon_i - 1)$, we have $\omega_i = [(\omega_p^2/(\varepsilon_\infty - \varepsilon_p)]^{1/2}$, $d\omega_i/d\varepsilon_m = {}^1/_2\omega_p(\varepsilon_\infty - \varepsilon_p)^{-3/2}$, and $\Delta\omega_{res}$ increases monotonically with the plasma frequency. Therefore, a higher plasma frequency ω_p will lead to a larger resonance shift for the same structure.

Equally important is the local electric field of the resonance mode $|\mathbf{E}_i(\mathbf{r})|$, which is solely decided by the geometry. In eq 9, it is evident that to achieve high sensitivity one needs to generate "hot spots" with a large local electric field intensity using special features such as nanometric corrugations, sharp corners, or narrow gaps.[1,9]

In practice, it is challenging to engineer the sensitivity of a plasmonic nanocavity sensor in quantitative fashion because the local field intensity at a "hot spot" is extremely sensitive to local geometical features. The authors have demonstrated in both theory and experiment that even nanometer corrugations can vary the local electric field intensity significantly.[38,39] Today, this issue can be partially addressed using newly developed numerical simulation techniques[38] and nanofabrication techniques, e.g., the helium ion microscope technique, which is capable of shaping nanostructures with a precision better than 5 nm.[40]

Another important property of $|\mathbf{E}_i(\mathbf{r})|$ is that it is inversely proportional to the volume of the plasmonic nanosensor *V*. Therefore, in order to improve the sensitivity, one needs to decrease the size of the sensor. Recent works have shown that, with new techniques, one can measure the resonance of Au particles as small as 5 nm,[41] much smaller than the size of current sensing devices. This opens up new possibilities for ultrasensitive plasmonic sensing devices. It is worth mentioning that a smaller volume will make the nanocavity more sensitive to the environmental fluctuations and consequently bring a higher noise level. This factor also needs to be taken into account in order to achieve the optimal limit-of-detection in practice.[2]

SUMMARY

In this work, we have developed a rigorous perturbation theory and derived a simple explicit expression for the NP-induced resonance frequency shifts of plasmonic nanocavities. We found that the resonance shifts are not only dependent on the local field intensity of the resonance modes, a well-known phenomenon in conventional dielectric microcavity-based sensors, but also proportional to $d\omega_i/d\varepsilon_{ca}$, a material dispersion-determined factor. Importantly, the relation is universal, applicable to all types of subwavelength nanocavities

dx.doi.org/10.1021/ph500355d | ACS Photonics 2015, 2, 144−150

made of dispersive materials. We verified this universal relation by numerically simulating 80 different cases with various nanocavity shapes, sizes, and materials. Moreover, we investigated the resonance shift in the context of energy and discussed the relation between the resonance shifts and optical forces. This result not only leads to a better understanding of the resonance shift for plasmonic nanocavities upon changes of their local environment but also provides general guidelines for analyzing and further developing efficient active plasmonic nanodevices.

■ ASSOCIATED CONTENT

Supporting Information

This material is available free of charge via the Internet at http://pubs.acs.org.

■ AUTHOR INFORMATION

Corresponding Author

*(W. Zhang) E-mail: zwh@nju.edu.cn. Phone: +86-25-83597175. Fax: +86-25-83597175.

Notes

The authors declare no competing financial interest.

■ ACKNOWLEDGMENTS

We gratefully acknowledge funding from the National Natural Science Foundation of China (Nos. 11021403 and 11374152), the Priority Academic Program Development (PAPD) of Jiangsu Higher Education Institutions, and the 1000 Young Talent Program of China.

■ REFERENCES

(1) Zhang, W. H.; Huang, L. N.; Santschi, C.; Martin, O. J. F. Trapping and sensing 10 nm metal nanoparticles using plasmonic dipole antennas. *Nano Lett.* **2010**, *10*, 1006−1011.

(2) Ament, I.; Prasad, J.; Henkel, A.; Schmachtel, S.; Sonnichsen, C. Single unlabeled protein detection on individual plasmonic nanoparticles. *Nano Lett.* **2012**, *12*, 1092−1095.

(3) Anker, J. N.; Hall, W. P.; Lyandres, O.; Shah, N. C.; Zhao, J.; Van Duyne, R. P. Biosensing with plasmonic nanosensors. *Nat. Mater.* **2008**, *7*, 442−453.

(4) Pala, R. A.; Shimizu, K. T.; Melosh, N. A.; Brongersma, M. L. Nonvolatile plasmonic switch employing photochromic molecules. *Nano Lett.* **2008**, *8*, 1506−1510.

(5) Cai, W.; White, J. S.; Brongersma, M. L. High-speed and power-efficient electrooptic plasmonic modulators. *Nano Lett.* **2009**, *9*, 4403−4411.

(6) Dionner, J. A.; Diest, K.; Sweatlock, L. A.; Atwater, H. A. PlasMOStor: a metal-oxide-Si field effect plasmonic modulator. *Nano Lett.* **2009**, *9*, 897−902.

(7) Pacifici, D.; Lezec, H.; Atwater, H. A. All-optical modulation by plasmonic excitation of CdSe quantum dots. *Nat. Photonics* **2007**, *1*, 402−406.

(8) Yao, Y.; Kats, M. A.; Genevet, P.; Yu, N.; Song, Y.; Kong, J.; Capasso, F. Broad electrical tuning of graphene-loaded plasmonic antennas. *Nano Lett.* **2013**, *13*, 1257−1264.

(9) Unger, A.; Rietzler, U.; Berger, R.; Kreiter, M. Sensitivity of crescent-shaped metal nanoparticles to attachment of dielectric colloids. *Nano Lett.* **2009**, *9*, 2311−2315.

(10) Sherry, L. J.; Jin, R. C.; Mirkin, C. A.; Schatz, G. C.; Van Duyne, R. P. Localized surface plasmon resonance spectroscopy of single silver triangular nanoprisms. *Nano Lett.* **2006**, *6*, 2060−2065.

(11) Zhang, S.; Bao, K.; Halas, N. J.; Xu, H.; Nordlander, P. Substrate-induced Fano resonances of a plasmonic nanocube: a route to increased-sensitivity localized surface plasmon resonance sensors revealed. *Nano Lett.* **2011**, *11*, 1657−1663.

(12) Sherry, L. J.; Chang, S. H.; Schatz, G. C.; Van Duyne, R. P.; Wiley, B. J.; Xia, Y. N. Localized surface plasmon resonance spectroscopy of single silver nanocubes. *Nano Lett.* **2005**, *5*, 2034−2038.

(13) Hao, F.; Sonnefraud, Y.; Van Dorpe, P.; Maier, S. A.; Halas, N. J.; Nordlander, P. Symmetry breaking in plasmonic nanocavities: subradiant LSPR sensing and a tunable Fano resonance. *Nano Lett.* **2008**, *8*, 3983−3988.

(14) Sun, Y. G.; Xia, Y. N. Increased sensitivity of surface plasmon resonance of gold nanoshells compared to that of gold solid colloids in response to enviromental changes. *Anal. Chem.* **2002**, *74*, 5297−5305.

(15) Chen, H. J.; Kou, X. S.; Yang, Z.; Ni, W. H.; Wang, J. F. Shape- and size-dependent refractive index sensitivity of gold nanoparticles. *Langmuir* **2008**, *24*, 5233−5237.

(16) Acimovic, S. S.; Ortega, M. A.; Sanz, V.; Berthelot, J.; Garcia-Cordero, J. L.; Renger, J.; Maerkl, S. J.; Kreuzer, M. P.; Quidant, R. LSPR chip for parallel, rapid, and sensitive detection of cancer markers in serum. *Nano Lett.* **2014**, *14*, 2636−2641.

(17) Ruemmele, J. A.; Hall, W. P.; Ruvuna, L. K.; Van Duyne, R. P. Localized surface plasmon resonance imaging instrument for multiplexed biosensing. *Anal. Chem.* **2013**, *85*, 4560−4566.

(18) Antosiewicz, T. J.; Apell, S. P.; Claudio, V.; Kall, M. A simple model for the resonance shift of localized plasmons due to dielectric particle adhesion. *Opt. Express* **2012**, *20*, 524−533.

(19) Unger, A.; Kreiter, M. Analyzing the performance of plasmonic resonators for dielectric sensing. *J. Phys. Chem. C* **2009**, *113*, 12243−12251.

(20) Piliarik, M.; Homola, J. Surface plasmon resonance (SPR) sensors: approaching their limits? *Opt. Express* **2009**, *17*, 16505−16517.

(21) Arnold, S.; Khoshsima, M.; Teraoka, I.; Holler, S.; Vollmer, F. Shift of whispering-gallery modes in microspheres by protein adsorption. *Opt. Lett.* **2003**, *28*, 272−274.

(22) Johnson, S. G.; Ibanescu, M.; Skorobogatiy, M. A.; Weisberg, O.; Joannopoulos, J. D.; Fink, Y. Perturbation theory for Maxwell's equations with shifting material boundaries. *Phys. Rev. B* **2002**, *65*, 066611.

(23) Joannopoulos, J. D.; Johnson, S. G.; Winn, J. N.; Meade, R. D. *Photonic Crystals*, 2d ed.; Princeton University Press, 2008.

(24) Zhao, L.; Yu, N. Modulation of mid-infrared light using graphene-metal plasmonic antennas. *Appl. Phys. Lett.* **2013**, *102*, 131108.

(25) Wang, F.; Shen, Y. R. General properties of local plasmons in metal nanostructures. *Phys. Rev. Lett.* **2006**, *97*, 206806.

(26) Raman, A.; Fan, S. Perturbation theory for plasmonic modulation and sensing. *Phys. Rev. B* **2011**, *83*, 205131.

(27) Zhang, W. H.; Gallinet, B.; Martin, O. J. F. Symmetry and selection rules for localized surface plasmon resonances in nanostructures. *Phys. Rev. B* **2010**, *81*, 233407.

(28) Gu, Y.; Chen, L. L.; Zhang, H. X.; Gong, Q. H. Resonance capacity of surface plasmon on subwavelength metallic structures. *Europhys. Lett.* **2008**, *83*, 27004.

(29) Stockman, M. I.; Faleev, S. V.; Bergman, D. J. Localization versus delocalization of surface plasmons in nanosystems: Can one state have both characteristics? *Phys. Rev. Lett.* **2001**, *87*, 167401.

(30) Fuchs, R. Theory of the optical properties of ionic crystal cubes. *Phys. Rev. B* **1975**, *11*, 1732−1740.

(31) Martin, O. J. F.; Girard, C.; Dereux, A. Generalized field propagator for electromagnetic scattering and light confinement. *Phys. Rev. Lett.* **1995**, *74*, 526−529.

(32) Zhang, W. H.; Fischer, H.; Schmid, T.; Zenobi, R.; Martin, O. J. F. Mode-selective surface-enhanced Raman spectroscopy using nanofabricated plasmonic dipole antennas. *J. Phys. Chem. C* **2009**, *113*, 14672−14675.

(33) Taflove, A.; Hagness, S. C. *Computational electrodynamics: the finite-difference time-domain method*, 3rd ed.; Artech: Boston, 2005.

(34) Jin, J.-M. *The Finite Element Method in Electromagnetics*, 2nd ed.; Wiley-IEEE Press, 2002.

(35) Lee, S.-W.; Lee, K.-S.; Ahn, J.; Lee, J.-J.; Kim, M.-G.; Shin, Y.-B. Highly sensitive biosensing using arrays of plasmonic Au nanodisks realized by nanoimprint lithography. *ACS Nano* **2011**, *5*, 897−904.
(36) Wu, P. C.; Sun, G.; Chen, W. T.; Yang, K.-Y.; Huang, Y.-W.; Chen, Y.-H.; Huang, H. L.; Hsu, W.-L.; Chiang, H. P.; Tsai, D. P. Vertical split-ring resonator based nanoplasmonic sensor. *Appl. Phys. Lett.* **2014**, *105*, 033105.
(37) Landau, L. D.; Lifshitz, E. M. *Electrodynamics of Continuous Media*; Pergamon: Oxford, 1984.
(38) Kern, A. M.; Martin, O. J. F. Excitation and reemission of molecules near realistic plasmonic nanostructures. *Nano Lett.* **2011**, *11*, 482−487.
(39) Zhang, W. H.; Cui, X. D.; Yeo, B.-S.; Schmid, T.; Hafner, C.; Zenobi, R. Nanoscale roughness on metal surfaces can increase tip-enhanced Raman scattering by an order of magnitude. *Nano Lett.* **2007**, *7*, 1401−1405.
(40) Scholder, O.; Jefimovs, K.; Shorubalko, I.; Hafner, C.; Sennhauser, U.; Bona, G.-L. Helium focused ion beam fabricated plasmonic antennas with sub-5 nm gaps. *Nanotechnology* **2013**, *24*, 395301.
(41) Lindfors, K.; Kalkbrenner, T.; Stoller, P.; Sandoghdar, V. Detection and spectroscopy of gold nanoparticles using supercontinuum white light confocal microscopy. *Phys. Rev. Lett.* **2004**, *93*, 037401.